



Significant grain refinement and enhanced mechanical properties of 6070 Al alloy via Ti/Sr addition and hot extrusion

M. Eamy^{*1}, B. Pourbahari², M. Mostafapour¹

¹School of Metallurgy and Materials Engineering, College of Engineering, University of Tehran, Tehran, Iran.

²Department of Materials Science and Engineering, McMaster University, Hamilton, Ontario, Canada.

Received: 9 September 2020; Accepted: 6 November 2020

* Corresponding author email: emamy@ut.ac.ir

ABSTRACT

The effects of Al-5Ti-1B and Al-10Sr master alloys on the microstructure and tensile properties of extruded 6070 Al alloy have been investigated in current research. Different amounts of Al-5Ti-1B and Al-10Sr master alloys were added to provide 0.01-0.5 wt.% of each element (Ti/Sr) in the alloy before homogenization, extrusion and heat treatment process. After adding 0.03 wt.% Ti and 0.03 wt.% Sr to the alloy separately, reduction in the average grain size was found to be %83 and eutectic Si changed from needle shape to fine fibrous morphology. Although the combined addition of Al-5Ti-1B and Al-10Sr increased slightly the grain size of the alloy, there was a considerable improvement in tensile properties for the extruded and T6-heat treated specimens. Further improvement in tensile strength was achieved after T6 heat treatment for 0.1 wt% Sr + 0.03% Ti added specimens in which ultimate tensile strength (UTS) showed the highest value (410 MPa). Fracture surface examinations revealed that hot extrusion process changes the mode of fracture from brittle in the as-cast condition to a more ductile form.

Keywords: 6070 Al alloy; Grain refinement; Modification; Extrusion.

1. Introduction

Aluminum alloys (6000 series) are widely used for structural applications due to their moderate strength, excellent formability, very good corrosion resistance and weldability, as well as the low cost, a unique feature is their great extrudability, making it possible to produce relatively complex shapes with good surface quality [1]. The main alloying elements in 6xxx series alloys are Si and Mg, which form precipitation of the Mg₂Si phase during aging treatment for improving mechanical properties of the alloy [2].

Among 6000 Al alloys, 6070 alloy has rather high strength and moderate ductility after hot deformation and T6 heat treatment. But, its

strength is lower than that of 2000 and 7000 series aluminum alloys. From several techniques which can be used to enhance the toughness (UTS and El.%) of Al-Si-Mg alloys, such as 6070 alloy, grain refinement and Si crystal modification seem to play a crucial role alongside the application of extrusion process and heat treatment.

Grain refining not only improves metallurgical characteristics and mechanical properties of the alloy but also facilitates subsequent mechanical forming processing [3]. From different kinds of grain refiners for Al alloys (i.e. Al-Ti, Al-Ti-B, Al-B and Al-TiC master alloys), Al-5Ti-1B is widely used in industrial applications [4-6]. The addition of grain refiner promotes the formation

of fine equiaxed grain structure by heterogeneous nucleation [7] and suppressing columnar grain growth [6]. In the heterogeneous nucleation process, an increase in either number density or nucleant potency of the nucleant particles enhances the nucleation rate, resulting in effective grain refining action [8, 9]. In contrast, the contribution of solute depends on its segregation in front of the liquid-solid interface as well as the driving force which is provided by constitutional undercooling to activate further nucleation on the substrates[10].

Furthermore, in Al-Mg-Si alloys the presence of coarse silicon with needle-like morphology is undesirable, resulting in poor mechanical properties. Several reports have shown the modifying effect of some metallic elements such as Na [11], Ca [12], Sc [13] and Sr [14] for morphological change of Si from needles to fine fibrous.

Li et al. [15] reported that when Al-10%Sr is added into an Al-Si-Cu melt together with Al-3%Ti- 4%B (at the holding temperature of 725°C), the precipitation of B from (Al,Ti)B₂ in Al-3%Ti-4wt.%B alloy and Sr from Al₄Sr in Al-10%Sr alloy results in the formation of SrB₆, which has a very high melting temperature of about 2500 °C [15]. The weight ratio of Sr to B in SrB₆ is 1.35:1, therefore, the consumption of Sr is larger than that of B in the precipitation process. Producing less SrB₆ and more dissolved B, consequently resulted in smaller grain size.

Lu and Dahle [16] have reported that with the addition of Al-1.5Ti-1.5B for grain refining and Sr for microstructural modification to the A356 molten alloy, the alloy loses its Sr much more quickly, particularly in the initial stage after addition, compared to a melt treated with only with Al-5Ti-1B. This explains the quick loss of eutectic modification in the Al-1.5Ti-1.5B treated melt, i.e. there is insufficient free Sr in the melt to modify all the eutectic Si. It is well known that molten Al-Si alloys can lose their Sr through surface oxidation and/or vaporization [17].

Samuel et al. [18] have also investigated the effect of combined addition of silicon modifier and grain refiners, i.e., Sr-B interaction on the tensile properties and impact toughness of the A356.2 casting alloy. An artificial ageing treatment (T6) is a universally accepted procedure to strengthen this series of alloy[19]. During artificial aging, a supersaturated solid solution decomposes as Mg and Si atoms are attracted first to themselves

(cluster), then to each other (co-cluster) to form precipitates of GP zones. Such zones either further evolve directly to a phase β' and then to a number of other metastable phases. The sequence depends on the Mg, Si content, the presence of additional elements such as Cu, Mn, Fe and the temperatures applied. The final equilibrium phase β is reached for higher temperatures only [20].

The aim of current research is to refine the microstructure of the 6070 alloy by adding Al-5Ti-1B grain refiner and Al-10Sr modifier. Concerning this, an effort was made to determine the optimized amounts of Ti and Sr and their combined effects on the microstructure and mechanical properties of 6070 alloy before and after hot extrusion process and T6 heat treatment.

2. Experimental procedure

2.1. Processing

An electrical resistance furnace was employed to prepare the primary ingots of 6070 alloy by the use of industrially pure Al (> 99.8%), Si (> 99.2%), and Mg (> 99.9%). The chemical composition of the 6070 Al alloy studied in this work has been shown in Table 1.

Afterwards, primary ingots were cut to small pieces for remelting in a small SiC crucible (1 Kg capacity). When the temperature reached 750±5 °C, Al-5Ti-1B and Al-10Sr master alloy were added into the melt to obtain different amounts of Ti or Sr (0.01, 0.03, 0.05, 0.1, 0.3 and 0.5 wt.%) in the alloy. Master alloys were first added individually to obtain their optimized conditions on the alloy macro- and microstructure and then they were tested simultaneously. Then, the melts were stirred manually with a silica rod to provide full mixing. Finally, the alloys with different compositions were cast into a preheated ductile iron mold (100 °C) to prepare cylindrical specimens (Fig. 1a).

Some specimens were tested in as-cast condition and the rest were subjected to homogenizing heat treatment (at 560 °C for 8 h), followed by slow cooling in the furnace to room temperature. Hot extrusion process was applied in a direct mode on a 100 tons hydraulic press at a ram speed of 1 mm/s with the extrusion ratio of 18:1 at 400 °C.

Some hot extruded specimens were subjected to T6 treatment. For this purpose, they were

Table 1- Chemical composition of the alloy in the study (wt.%)

| Al | Mg | Si | Mn | Cu | Fe |
|------|------|------|------|------|------|
| Bal. | 0.86 | 1.43 | 0.73 | 0.35 | 0.15 |

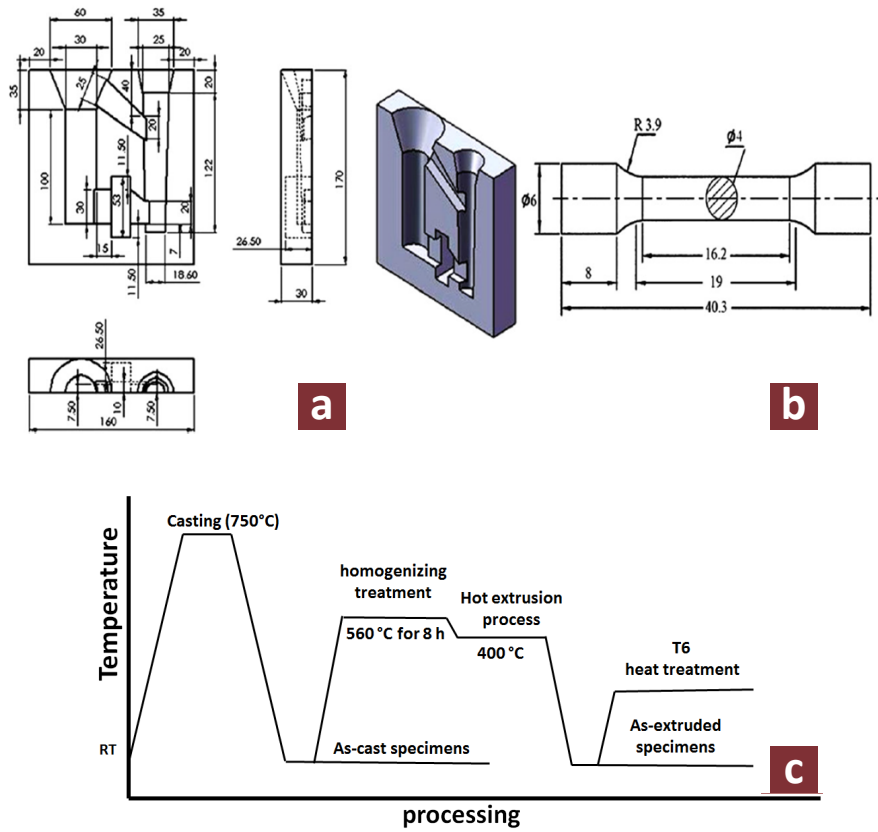


Fig. 1- Schematic illustrations of (a) casting mould (mm), (b) the tensile test specimen (mm), and (c) the processing route.

solution treated in an accurate electrical furnace at 540 °C for 6 h, then quenched in water to room temperature, and finally aged at 180 °C for 12 h prior to air cooling.

2.2. Characterization

The specimens were ground and polished according to the standard metallographic procedure and etched by Keller’s reagent (2 ml HF, 3 ml HCl, 5 ml HNO₃ and 190 ml H₂O) to reveal the microstructure.

The microstructural characteristics of the specimens were examined via optical microscopy (OM), scanning electron microscopy performed in a Vega©Tescan SEM assembled with an energy dispersive X-ray (EDX) analysis accessory and field emission scanning electron microscopy (FESEM), MIRA3 Tescan. In this work, the grain size of cast specimens was measured by the linear intercept method according to ASTM E112-13 standard.

The tensile specimen was prepared according to ASTM: E8-04 standard (Fig. 1b). Tensile testing was carried out at room temperature by a computerized

testing machine (SANTAM STM-20) at the constant cross-head speed of 0.1 mm/min. Each tensile test was repeated once. Finally, the fracture surfaces of tensile test specimens were also examined with the electron microscopy.

3. Results and discussion

3.1. Structural studies in as-cast condition

3.1.1. Effect of separate Ti/Sr additions

Table 2 and Fig. 2 illustrate cast specimen codes and the results of individual addition of Ti and Sr, using Al-5Ti-1B and Al-10Sr master alloys, on the average grain size of the 6070 Al alloy. Fig. 3 also exhibits typical macrostructures of small billets before and after refinement and modification by Ti and Sr additions.

The study of refined and modified specimens showed different microstructural features. To obtain a proper structure and also better tensile properties, it was necessary to find optimum levels of added refiner and modifier. From Fig. 2 and Table 2, it is seen that by individual addition of 0.03 wt.% Ti and 0.03 wt.% Sr to the alloy, average grain size decreases

from 893 μm to 156 μm and 515 μm , respectively. It can be seen that Ti addition is more effective than Sr in grain refinement of the alloy. According to the previous investigations, alloy refinement or modification generally takes place in two types: (1) heterogeneous nucleation, i.e., the modifying elements or their containing compounds act as the heterogeneous nucleus; (2) poisoning effect, i.e., modifying elements absorb the forehead of growth and restrict the crystal growth. As expected, the main influence of Sr addition is its modification effect on Si crystals of Al-Si alloys [2]. It is well established that by adding Al-10Sr master alloy, the free Sr is available in the liquid resulting from the dissolution of Al_4Sr intermetallic which can restrict the grain growth during solidification as well.

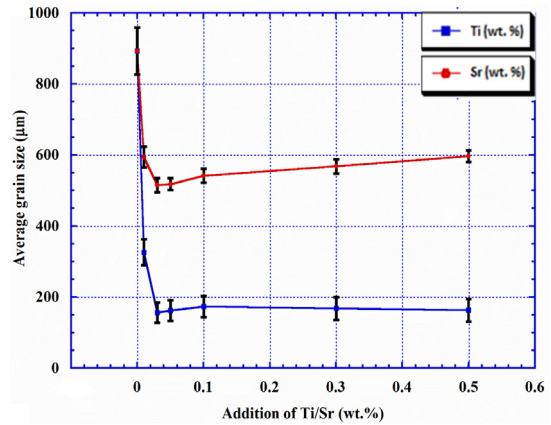


Fig. 2- The average grain size variations with different amounts of Ti(+B) or Sr before extrusion.

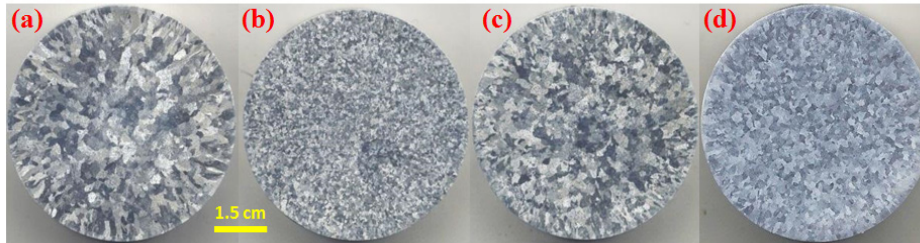


Fig. 3- Optical photograph of alloy containing: (a) without Ti(+B) and Sr, (b) 0.03 wt.% Ti(+0.006), (c) 0.03 wt.% Sr and (d) 0.03 wt.% Ti(+0.006) + 0.03 wt.% Sr.

Table 2- Grain size variation of specimens containing different amounts of Ti and Sr in as-cast condition

| Sample No. | Ti (+B) wt.% | Sr wt.% | Grain Size (μm) | Std. dev. (μm) |
|------------|--------------|---------|------------------------------|-----------------------------|
| Al-C | - | - | 893 | 66 |
| T01-C | 0.01(+0.002) | - | 326 | 36 |
| T03-C | 0.03(+0.006) | - | 156 | 28 |
| T05-C | 0.05(+0.01) | - | 162 | 29 |
| T10-C | 0.10(+0.02) | - | 173 | 33 |
| T30-C | 0.30(+0.06) | - | 168 | 35 |
| T50-C | 0.50(+0.10) | - | 163 | 30 |
| S01-C | - | 0.01 | 594 | 50 |
| S03-C | - | 0.03 | 515 | 34 |
| S05-C | - | 0.05 | 518 | 29 |
| S10-C | - | 0.10 | 542 | 31 |
| S30-C | - | 0.30 | 568 | 35 |
| S50-C | - | 0.50 | 597 | 26 |
| TS03- C | 0.03(+0.006) | 0.03 | 258 | 20 |
| TS05- C | 0.03(+0.006) | 0.05 | 287 | 26 |
| TS10- C | 0.03(+0.006) | 0.10 | 304 | 22 |
| ST05- C | 0.05(+0.01) | 0.03 | 233 | 24 |
| ST10- C | 0.10(+0.02) | 0.03 | 224 | 21 |

Al: Ti and Sr free specimen

C: as-cast condition

T01: specimen containing 0.01 wt.% Ti

S10: specimen containing 0.10 wt.% Sr

TS05: specimen containing both Ti and Sr, Ti=0.03 wt.%, Sr=Variable

ST10: specimen containing both Ti and Sr, Sr=0.03 wt.%, Ti=Variable

On the other hand, it has been shown that $TiAl_3$ intermetallic, in Al-5Ti-1B master alloy, not only acts as heterogeneous nucleation site, but also its dissolution provides solute Ti in the melt which can retard grain growth during solidification process [6]. However, no further grain refining occurs with the use of excess amounts of Ti, as seen in Fig. 2. Maxwell and Hellawell have reported that the number of nuclei more than an optimum amount is not necessary for nucleation and will be pushed into the grain boundary by the advance of the freezing front [21]. Fig. 4 depicts typical microstructures of 6070 Al alloy specimens before and after Ti and Sr additions.

From Fig. 4a, it is seen that Ti/Sr free specimens possess dendritic structures containing Al-rich α phase. The EDS analysis of Ti/Sr free alloy shows new intermetallics (as depicted in Fig. 5). Similarly, some reports have shown that Al_9Mn_3FeSi and Si eutectic are these new phases [22].

The addition of Al-5Ti-1B grain refiner reduces the length of primary α -Al dendrites (Fig. 4b), but, by adding 0.03 wt.% Sr to the alloy a rosette-like morphology appears in the microstructure instead of long dendrites (Fig. 5). Altering the morphology of primary dendritic structure by adding refiners/modifiers has been reported by several investigators [23, 24].

To observe the distribution of constituents in the microstructure, SEM back-scattered electron images of as-cast specimens are shown in Fig. 4. In comparison with the structure of Ti/Sr free

samples (Fig. 4a), the more uniform and finer microstructure is seen in Ti added specimen (Fig. 4b).

Secondary electron images of the specimens, shown in Fig. 6, clearly reveal that silicon particle size is changed from large particles to fine fibers.

As shown in this Fig. 6b, by adding 0.03 wt.% Sr to the alloy, the morphology of eutectic Si changes from needles to fine fibers (Fig. 6b) which is in agreement with the theoretical standpoint that for complete modification of eutectic Si the critical amount of Sr is relatively low [25].

The modifying effect of Sr on Si crystal is well known in literature [26, 27] according to an impurity induced twinning modified Si fibers include more twins than the unmodified ones and have a rough micro-faceted surface and each surface imperfection is a potential site for branching. Therefore, the silicon fibers tend to bend, curve and split in the chemically modified eutectic to create a fine microstructure. Lu and Hellawell [28] believe that a growth twin is generated at the interface when the atomic radius of the element has the accurate size relative to the radius of Si ($r_{\text{element}} : r_{\text{Si}} = 1.65$) that Sr element is found to be in the atomic radius range proposed to cause chemical modification.

As a result of the reduction in the average grain size by (Fig. 3). Due to the obtained experimental results, the optimized condition for grain refining and modification is attained by adding 0.03 wt.% Ti and 0.03 wt.% Sr, separately.

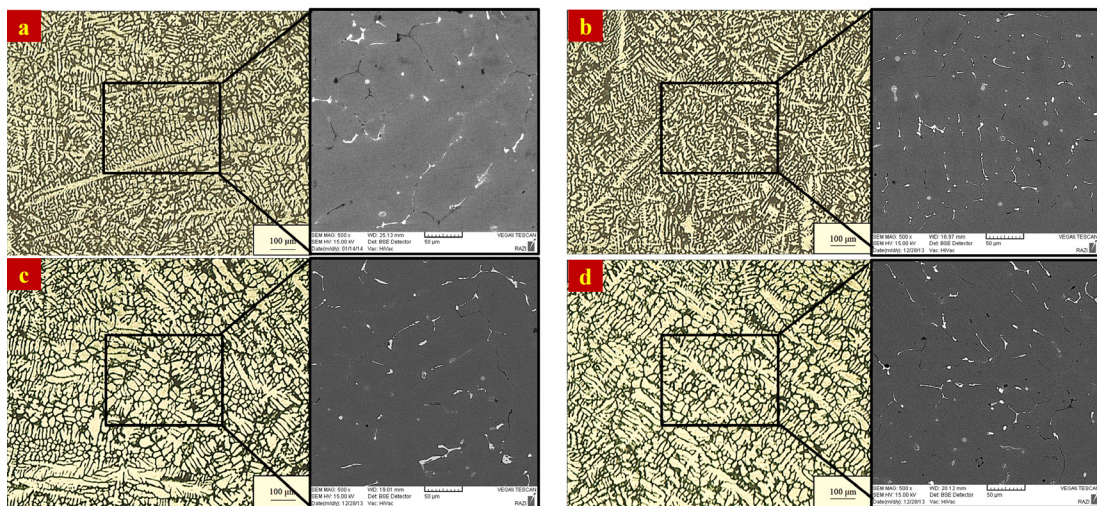


Fig. 4- The optical microscope images of typical microstructures of 6070 alloy before extrusion: (a) without Ti(+B) and Sr, (b) 0.03 wt.% Ti(+0.006), (c) 0.03 wt.% Sr and (d) 0.03 wt.% Sr + 0.03 wt.% Ti(+0.006).

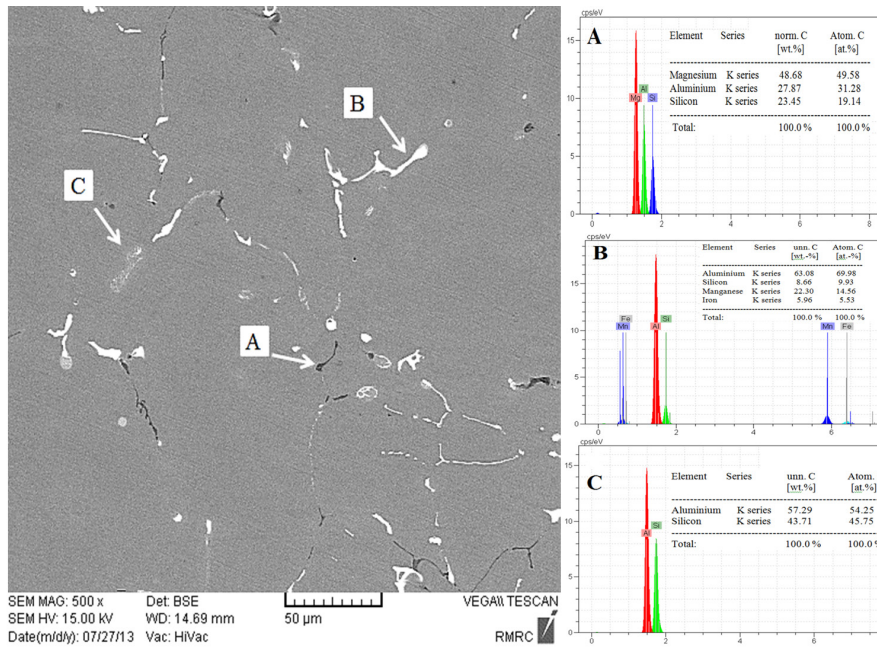


Fig. 5- SEM image of second phases distribution of alloy before extrusion without Ti(+B) and Sr with relative EDS point analysis.

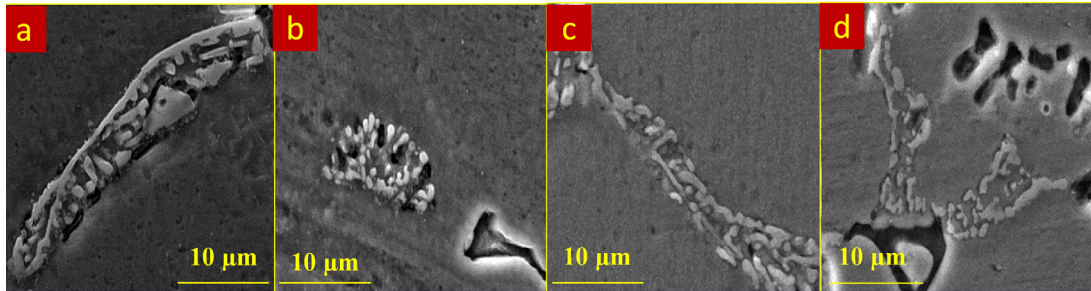


Fig. 6- SEM images of eutectic Si of the alloy with different Ti(+B) and Sr additions before extrusion: (a) free Ti (+B) and Sr, (b) 0.03 wt.% Sr, (c) 0.03 wt.% Sr + 0.05 wt.% Ti (+0.01) and (d) 0.03 wt.% Sr + 0.1 wt.% Ti (+0.02).

3.1.2. Effect of combined Ti and Sr additions

From Fig. 4d, it is observed that simultaneous addition of Al-5Ti-1B and Al-10Sr to the 6070 Al alloy, similar to Sr-modified specimens (Fig. 4d), the fully dendritic morphology of primary α -Al has been changed to an approximately rosette-like shape.

Table 2 also depicts the effect of combined addition of Ti and Sr on the average grain size of the alloy. From Table 2, it can be seen that Sr addition acts against Ti refinement and increase the grain size of the cast specimens seriously. This coarsening behavior of grains can be due to the formation of SrB_6 through the reaction between B and Sr which are mainly introduced from the dissolution of TiB_2 and Al_4Sr respectively [29]. The reaction between Sr

and B may lead to the reduction of the indispensable boron atoms for grain refinement. The incident of this interaction has a harmful effect on the efficiency of added grain refiners, therefore a higher level of grain refiner would be demanded to acquire a given grain size [18].

On the contrary, by adding Al-5Ti-1B master alloy to Sr-modified specimens, the grain size decreases, showing the apparent beneficial effect of the grain refinement on Sr-modified alloy. Table 2 also depicts that by adding more Al-5Ti-1B master alloy and accordingly boron content, the grain refining effect restores, which may be due to the attainable increased number of TiB_2 and Al_3Ti particles.

Fig. 6c-d shows SEM images of eutectic Si, when

Al-5Ti-1B and Al-10Sr are added simultaneously. Compared to Fig. 6b, it is evident that when Al-5Ti-1B is added into the Sr-modified specimens, the eutectic Si has become partially modified which will be more pronounced when boron content increases (Fig. 6d). Since the modification effect of Al-10Sr master alloy is high in dissolved condition, by adding Al-5Ti-1B master alloy, the formation of SrB_6 which consumes more atomic Sr results in reduced Sr concentration for complete modification of eutectic Si [15]. This result implies harmful effect of Al-5Ti-1B addition on Sr-modified 6070 alloy. Therefore, a higher level of Al-10Sr master alloy

is needed to obtain good modification effect when the Sr-modified alloy is treated by Al-5Ti-1B [15].

As shown in Fig. 4d, the combined addition of Ti and Sr improves the uniformity of the alloy microstructure. As mentioned above, it can be attributed to the reduction in grain size when Ti and Sr are added simultaneously (Table 2).

3.2. Microstructural study after hot extrusion

Fig. 7 shows microstructure of specimens with different amounts of Ti and Sr after hot extrusion and T6 heat treatment which applied after hot extrusion.

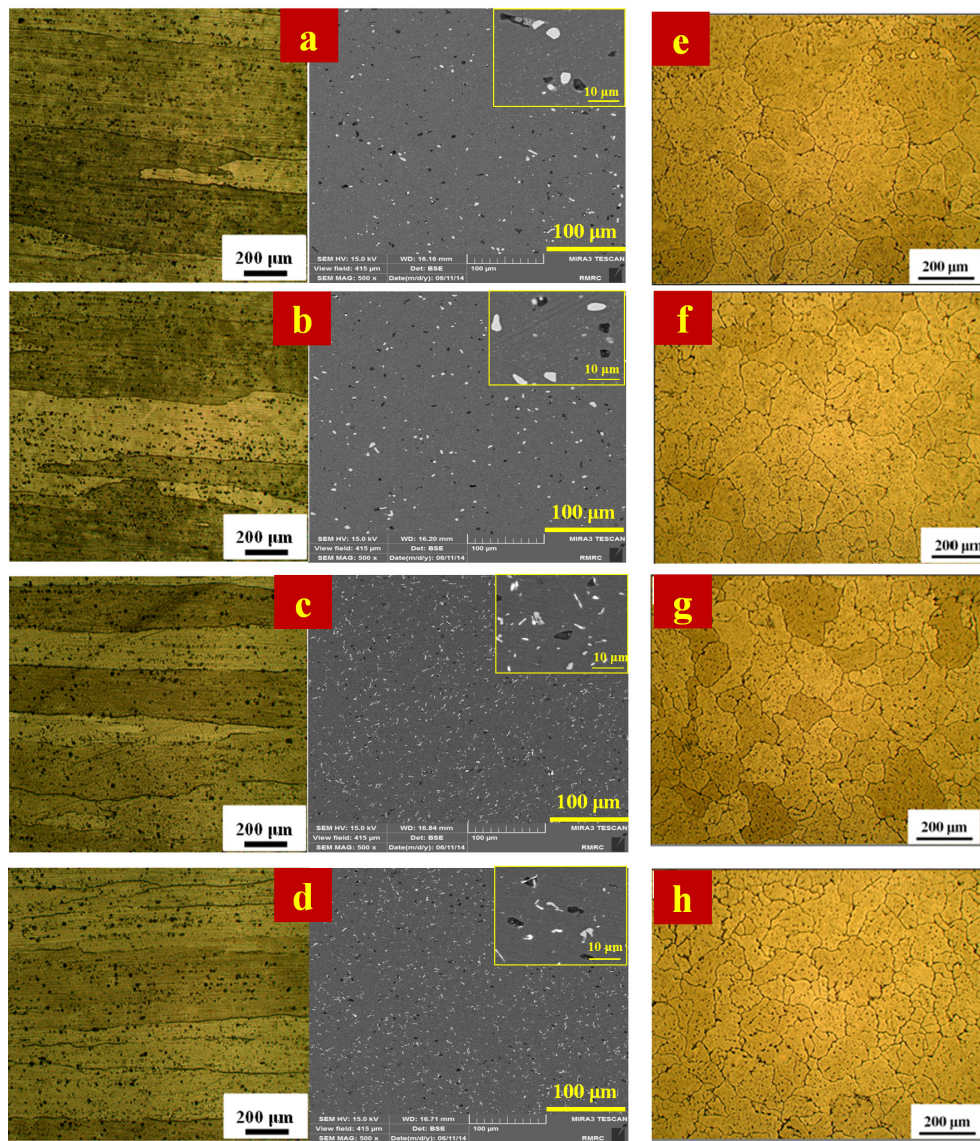


Fig. 7- SEM images of second phases distribution of alloy after (a-d) extrusion and (e-h) heat treatment: (a-e) without Ti(+B) and Sr, (b-f) 0.03 wt.% Sr, (c-g) 0.03 wt.% Ti(+0.006) and (d-h) 0.03 wt.% Sr + 0.03 wt.% Ti(+0.006).

As illustrated in Fig. 7, the homogenization treatment and hot extrusion process have a significant effect on the size reduction and distribution of the constituents in the microstructure. During hot extrusion, particles of intermetallic phases arrange in positions parallel to the direction of plastic deformation which encourages the formation of the band structure. As shown in Fig. 7, severely elongated grains are observed in all extruded bar which suggests that dynamic or static recovery be the main restoration process during or after the hot extrusion. It is thought, therefore, the recrystallization does not proceed at this central region.

Moreover, as shown in Fig. 7, it can be concluded that the specimens containing either Ti or both Ti and Sr demonstrate more uniform structure after the hot extrusion process. This result also indicates that the post-extrusion microstructure can be influenced by pre-extrusion microstructure.

Microstructural evolutions after heat treatment of the extruded bar are shown in Figs. 7 (e-h). It can be seen that fine equiaxed grains evolved in samples suggest that recrystallization occurs during the heat treatment. It can be observed that the sample containing Ti, the grain size is lower than the sample without Ti addition because $TiAl_3$ particles hinder recrystallization of grain boundaries during extrusion and solution treatments in Ti-refined specimen.

3.3. Tensile properties

3.3.1. Individual addition of Ti and Sr

Fig. 8 demonstrates tensile test results of as-cast specimens containing different amounts of Ti and Sr

which are added individually to the alloy.

From Fig. 8, it can be observed that Ti addition, from 0.00 wt.% to 0.03 wt.%, results in UTS enhancement from 212 MPa to 236 MPa and elongation improvement from 4.2% to 6.5%. The main reason for this improvement is high probably due to the reduction in the grain size of the alloy, providing finer structure and more uniform distribution of the constituents, as shown in Fig. 4b [30]. At high Ti levels (> 0.03 wt.%), UTS and elongation values decrease to some extent. Some research works have indicated that the formation of agglomerated $TiAl_3$ and TiB_2 in grain boundary regions is the main reason for this reduction [21]. During solidification, Ti segregates in front of liquid-solid interface and agglomeration of Ti containing particles is encouraged by adding more Ti. In this work, such agglomerated particles are illustrated in Fig. 9, related to a highly added Ti cast specimen.

It is known that this intermetallic may act as crack initiators, thereby diminishing mechanical properties.

Fig. 8 also depicts the addition of 0.03 wt.% Sr increases UTS and elongation percentage slightly. This can be attributed to the refinement of intermetallic compounds (Fig. 4c) and the modification of eutectic Si from needle shape to a fine fibrous morphology, as shown in Fig. 5b. Also, it can be seen that by further increase in the amount of Sr in the alloy from 0.03 wt.% to 0.5 wt.%, both UTS and elongation values are decreased slightly. These variations are in agreement with microstructural observations.

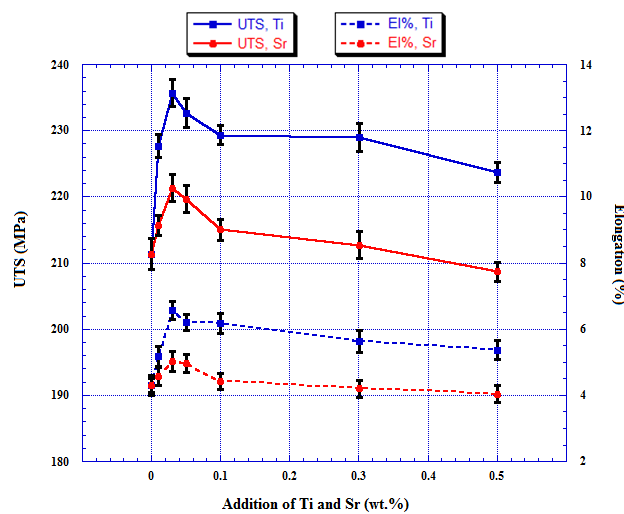


Fig. 8- The effect of Ti(+B) grain refiner and Sr modifier on UTS and El.% values before extrusion.

3.3.2. Simultaneous addition of Ti and Sr

Fig. 10 depicts the effect of Sr addition on tensile properties of 0.03 wt.% Ti-refined specimens in as-cast, extruded and heat treatment conditions.

It can be seen that Sr addition to Ti-refined specimens has a marginal effect on tensile properties of the alloy. It seems that Sr addition acts against Ti refinement and increase the grain size of the cast specimens seriously. This coarsening behavior of grains can be due to the formation of SrB6 through the reaction between B and Sr.

In contrast, by the addition of Ti to 0.03 wt.% Sr-modified specimens, UTS and elongation values increase. As mentioned before, by adding Al-5Ti-

1B master alloy to Sr-modified specimens, the grain size decreases, showing the apparent beneficial effect of the grain refinement on Sr-modified alloy (Fig. 11).

This advancement can be due to the decreased grain size and uniform dispersion of the constituents in the alloy. The highest UTS and elongation values are attained by adding 0.05 wt.% Ti to the 0.03 wt.% Sr specimen which intensifies from 221 MPa to 237 MPa and 5% to 6.9%, showing about 7% and 40% improvement, respectively.

The low elongation values in as-cast condition can be due to the microstructural features, showing large and coarse constitutions (Fig. 5).

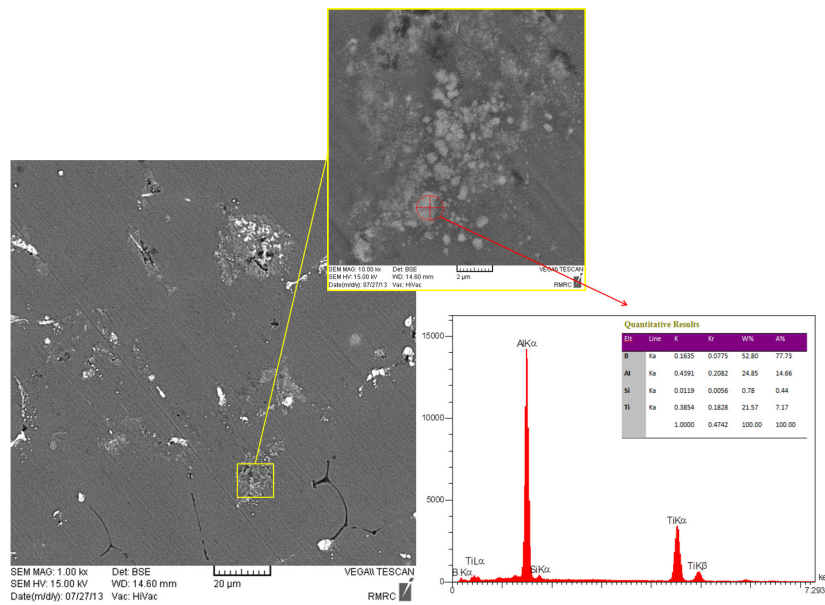


Fig. 9- Agglomeration of TiAl₃ and TiB₂ particles in large amount of Ti (0.5 wt.%).

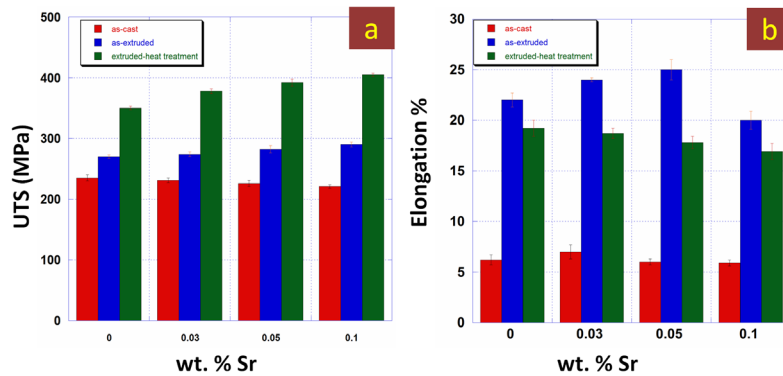


Fig. 10- Variation of tensile properties of the 0.03 wt.%Ti-refined specimen treated by Sr (a) UTS and (b) elongation.

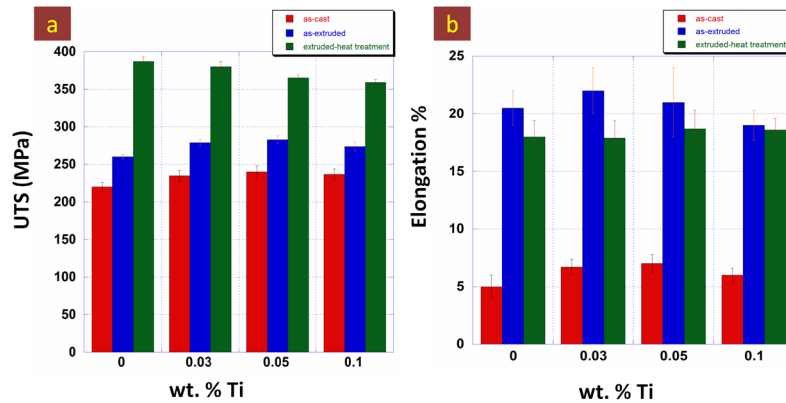


Fig. 11- Variation of tensile properties of the 0.03 wt%Sr-refined specimen treated by Ti(+B) (a) UTS and (b) El.%.

It is important to note that the presence of coarse intermetallic compounds in grain boundaries region act as high-stress concentration sites which provide preferable sites for crack nucleation and growth. Furthermore, with more precipitation of intermetallic compounds at the grain boundaries, the fracture mode shifts from predominantly transgranular to predominantly intergranular [31].

According to the results obtained from tensile testing, hot extrusion is an effective thermo-mechanical process in enhancing both UTS and elongation values of the alloy, as shown in Fig. 10 and Fig. 11. These results are also in agreement with microstructural observations, showing fine and uniform distribution of the constituents. As expected, the elimination of casting defects such as microshrinkage, after the hot extrusion process is helpful in such improvement [32].

From Fig. 10, it can be seen that Sr addition to the Ti-refined extruded alloy has margin effect on tensile properties; whereas Ti has a discernible influence on the Sr-modified specimens after extrusion, as seen in Fig. 11. This enhancement can be attributed to the fine and uniform structure of Sr-modified specimen in the presence of Ti after extrusion (Fig. 7d). A comparison between quantitative analysis of S03 and ST05 extruded specimens reveals that the addition of 0.05 wt.% Ti to the Sr-modified specimen improves UTS value of the alloy from 259 MPa to 281 MPa and elongation percentage from 18.6 to 21.5, presenting about 8% and 16% improvement, respectively.

Heat treatment process after hot extrusion enhances UTS values of the alloy considerably, but a reduction in elongation value after the applied heat treatment can be observed. It can be

due to the formation of equiaxed grains resulting from the recrystallization phenomenon which occurs during heat treatment (as shown in Fig. 10 and Fig. 11). The interesting result obtained from combining heat treatment process on 0.1 wt.% Sr added and Ti-refined specimen, in which UTS reaches to the highest value (410 MPa). In addition to this modifying effect, there is further evidence to indicate that Sr influences the Mg_2Si precipitation kinetics in 6000 series Al alloys [8] as well as in Al-Si-Mg foundry alloys [22]. In addition Al_3Ti particles hinder recrystallization of grain boundaries during extrusion and solution treatments in Ti-refined specimen. So, Ti-refined alloy has higher tensile properties. But in Sr-refined specimen, by increasing Ti content, no considerable changes are seen in the results of tensile properties.

3.4. Fractography

Typical fracture surfaces of the alloy after adding different amounts of Ti and Sr in as-cast, hot extruded and heat treatment conditions are shown in Fig. 12 and Fig. 13.

Examination of several fracture surfaces of selected cast specimens showed several cleavage facets of cleavage mode of fracture, as shown in Fig. 12.

Examination of several fracture surfaces of selected cast specimens showed a cleavage pattern with flat facets representing the Al-Si eutectic zone, as shown in Fig. 12. In these flat areas, the Si platelet might be torn off from the Al matrix, leaving a terrace with a smooth facet. These facets were more probably formed as a result of the fracture of brittle Si phase crystals and broken intermetallics (as shown in the enlarged area in

the top corner of Fig. 12a). Further observations at higher magnification also revealed that the number of dimples is low and there are some secondary cracks are seen on the fractured faces of the cast specimens, as shown by red arrows in Fig. 12. During microstructural observations, although very large plate-like Fe-bearing intermetallics were not found in the microstructures, some intermetallics with rather sharp edges were found in the cast state. Both intermetallics and Si particles encourage the initiation of the cracks on the sharp corners to reduce the toughness of the cast alloy. It seems that during loading, after initiation of the cracks on appropriate stress concentration sites, failure of the cast specimens can be taken place by an intergranular fracture path. Also, the propagation of cracks was associated with fracture of coarse particles in eutectic regions (Fig. 6). It has been noted that Si particle size and shape are parameters affecting the ductility of Al-Si alloys.

By increasing strain values, cracks tend to grow and coalesce at regions of localized strain. This can explain the low elongation values of the specimens before extrusion.

Fig. 12b shows the fracture surface of the alloy with 0.03 wt.% Sr. From Fig. 12b, it can be seen the appearance of cleavage fracture on the fracture

surface but, a few dimpling features are observed on the cleavage facets which show faint characteristics of quasi-cleavage fracture. It can be the result of morphological changes of Si crystals to fine and spherical shape by adding Sr to 6070 aluminum alloy (Fig. 6b).

It is evident from Fig. 12c that the fracture surface of Ti modified alloy in as-cast condition exhibits quasi-cleavage feature and a brittle fracture nature, in comparison with Sr modified alloy the amount of dimple is fewer in 0.03 wt.% Ti addition. But simultaneous addition of Ti and Sr leads to shows more uniform dimples (Fig. 12d), because of more homogeneous distribution of second phases, more refined and uniform grains and modified Si crystals which result in tensile properties improvement.

Fig. 13 clearly shows the topographic features of tensile fracture surfaces of 6070 Al alloy after extrusion and heat treatment.

The observed changes in the fracture surface depict a typical ductile fracture mode consisting of fine conical equiaxed dimples. In comparison with as-cast specimens in Fig. 12, the existence of deep and conical shape of dimples on hot-extruded specimens indicates higher ductility. This result is in agreement with the increased elongation values of the extruded specimens, as shown in Fig. 10 and

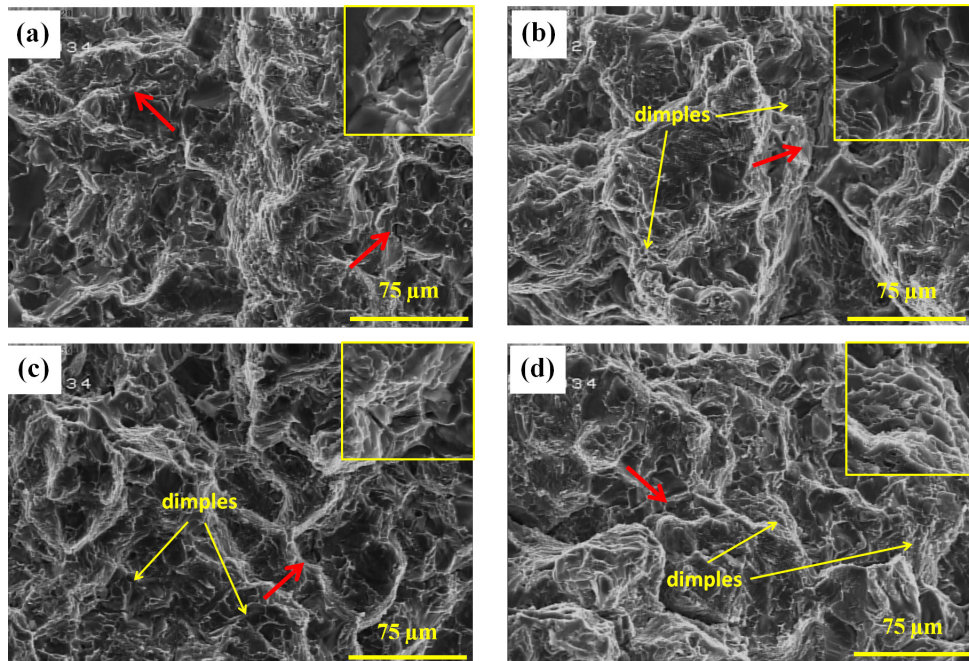


Fig. 12- SEM images of the fracture surface of alloy before extrusion: (a) without Ti and Sr, (b) 0.03 wt.% Sr, (c) 0.03 wt.% Ti and (d) 0.03 wt.% Sr + 0.05 wt.% Ti.

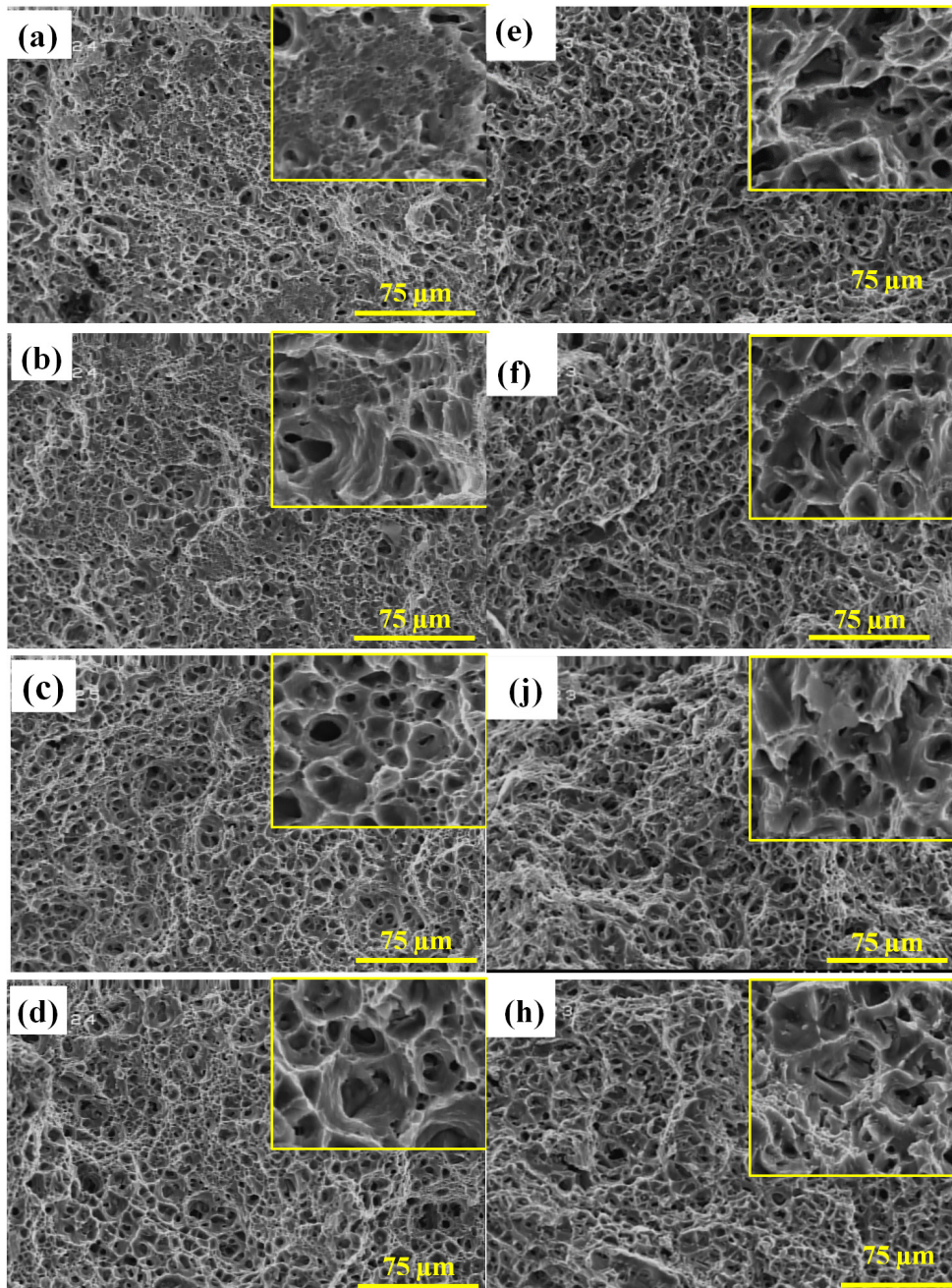


Fig. 13- SEM images of the fracture surface of alloy after extrusion(a-d) and heat treatment (e-h): (a-e) without Ti and Sr, (b-f) 0.03 wt.% Sr, (c-j) 0.03 wt.% Ti and (d-h) 0.03 wt.% Sr + 0.05 wt.% Ti.

Fig. 11. Enhancement in ductility of the alloy can be due to the observed homogeneity and uniform dispersion of intermetallic phases in the alloy structure, as shown in Fig. 7. The ductile fracture is determined by the size, number and distribution of dimples. Moreover, more homogeneity and deeper dimples reveal a higher ductility for such

alloys. By comparing the fracture surfaces of specimens in as-extruded and T6 heat treatment after extrusion conditions, it can be noted that T6 heat treatment encourages ductile fracture mode. As shown in Fig. 13e, the fracture face of the heat treated specimen demonstrates fully dimple-like appearance. So, more ductile behavior is expected

in heat treated alloy.

Examination of Ti/Sr-free specimen revealed some quasi-cleavage facets sporadically in isolated areas of the fracture surfaces, as shown in Fig. 13a.

It is noted that the addition of either Ti or both Ti and Sr not only increases the number of dimples but also introduces deeper and uniformly distributed dimples, as shown in Fig. 13 which result in the improved tensile properties.

4. Conclusions

This study aimed to determine the individual and combined effects of Al-5Ti-1B and Al-10Sr master alloys on the microstructure and mechanical properties of 6070 aluminum alloy before and after extrusion. The following results are:

(1) By individual addition of master alloys, similar Ti/Sr content (0.03 wt.%) is found for proper grain refinement and modification. The simultaneous addition of Al-5Ti-1B and Al-10 Sr can efficiently refine the grains of Al-Mg-Si alloy, however, the grains became slightly coarser than the condition in which Ti is used separately.

(2) The extruded alloys exhibit much higher UTS and elongation values compared to the as-cast alloys.

(3) No significant improvement in tensile properties of Ti-refined alloy treated by Sr is observed. In contrast, the addition of Ti to Sr-modified alloy increases the tensile properties before and after hot extrusion process. Further improvement in tensile strength was achieved after T6 heat treatment for 0.1 wt% Sr + 0.03% Ti added specimens, in which UTS showed the highest value (410 MPa).

(4) The fracture surfaces of the cast specimens reveal a brittle fracture mode, but after extrusion fracture mode is ductile, in agreement with elongation value enhancement of the alloy.

References

1. Troeger LP, Starke EA. Microstructural and mechanical characterization of a superplastic 6xxx aluminum alloy. *Materials Science and Engineering: A*. 2000;277(1-2):102-13.
2. Kori SA, Murty BS, Chakraborty M. Development of an efficient grain refiner for Al-7Si alloy and its modification with strontium. *Materials Science and Engineering: A*. 2000;283(1-2):94-104.
3. Murty BS, Kori SA, Chakraborty M. Grain refinement of aluminium and its alloys by heterogeneous nucleation and alloying. *International Materials Reviews*. 2002;47(1):3-29.
4. Xu C, Xiao W, Zhao W, Wang W, Shuji H, Hiroshi Y, et al. Microstructure and formation mechanism of grain-refining particles in Al-Ti-C-RE grain refiners. *Journal of Rare Earths*. 2015;33(5):553-60.
5. Yamauchi K, Kunimine T, Sato H, Watanabe Y. Grain Refinement of Al₃Ti Dispersed Aluminum Matrix Composites by Reaction Centrifugal Mixed-Powder Method. *MATERIALS TRANSACTIONS*. 2015;56(1):99-107.
6. Fan Z, Wang Y, Zhang Y, Qin T, Zhou XR, Thompson GE, et al. Grain refining mechanism in the Al/Al-Ti-B system. *Acta Materialia*. 2015;84:292-304.
7. Wang X, Liu Z, Dai W, Han Q. On the Understanding of Aluminum Grain Refinement by Al-Ti-B Type Master Alloys. *Metallurgical and Materials Transactions B*. 2015;46(4):1620-5.
8. Li P, Liu S, Zhang L, Liu X. Grain refinement of A356 alloy by Al-Ti-B-C master alloy and its effect on mechanical properties. *Materials & Design*. 2013;47:522-8.
9. Birol Y. Efficiency of binary and ternary alloys from Al-Ti-B system in grain refining aluminium foundry alloys. *International Journal of Cast Metals Research*. 2013;26(5):283-8.
10. Wang T, Gao T, Nie J, Li P, Liu X. Influence of carbon source on the microstructure of Al-Ti-C master alloy and its grain refining efficiency. *Materials Characterization*. 2013;83:13-20.
11. Li JH, Barrirero J, Engstler M, Aboufadh H, Mücklich F, Schumacher P. Nucleation and Growth of Eutectic Si in Al-Si Alloys with Na Addition. *Metallurgical and Materials Transactions A*. 2015;46(3):1300-11.
12. Ludwig TH, Schonhvd Dæhlen E, Schaffer PL, Arnberg L. The effect of Ca and P interaction on the Al-Si eutectic in a hypoeutectic Al-Si alloy. *Journal of Alloys and Compounds*. 2014;586:180-90.
13. Zhang W, Liu Y, Yang J, Dang J, Xu H, Du Z. Effects of Sc content on the microstructure of As-Cast Al-7wt.% Si alloys. *Materials Characterization*. 2012;66:104-10.
14. Liu X, Zhang Y, Beausir B, Liu F, Esling C, Yu F, et al. Twin-controlled growth of eutectic Si in unmodified and Sr-modified Al-12.7%Si alloys investigated by SEM/EBSD. *Acta Materialia*. 2015;97:338-47.
15. Li JG, Zhang BQ, Wang L, Yang WY, Ma HT. Combined effect and its mechanism of Al-3wt.%Ti-4wt.%B and Al-10wt.%Sr master alloy on microstructures of Al-Si-Cu alloy. *Materials Science and Engineering: A*. 2002;328(1-2):169-76.
16. Lu L, Dahle AK. Effects of combined additions of Sr and AlTiB grain refiners in hypoeutectic Al-Si foundry alloys. *Materials Science and Engineering: A*. 2006;435-436:288-96.
17. Closset B, Gruzleski JE. Structure and properties of hypoeutectic Al-Si-Mg alloys modified with pure strontium. *Metallurgical Transactions A*. 1982;13(6):945-51.
18. Samuel E, Golbahar B, Samuel AM, Doty HW, Valtierra S, Samuel FH. Effect of grain refiner on the tensile and impact properties of Al-Si-Mg cast alloys. *Materials & Design* (1980-2015). 2014;56:468-79.
19. Panigrahi SK, Jayaganthan R, Pancholi V. Effect of plastic deformation conditions on microstructural characteristics and mechanical properties of Al 6063 alloy. *Materials & Design*. 2009;30(6):1894-901.
20. I. Polmear, *Light Alloys*, Butterworth-Heinemann, Amsterdam 2006 (4th ed.).
21. Maxwell I, Hellawell A. A simple model for grain refinement during solidification. *Acta Metallurgica*. 1975;23(2):229-37.
22. Mulazimoglu MH, Zaluska A, Paray F, Gruzleski JE. The effect of strontium on the Mg₂Si precipitation process in 6201 aluminum alloy. *Metallurgical and Materials Transactions A*. 1997;28(6):1289-95.
23. Nafisi S, Ghomashchi R. Grain refining of conventional and semi-solid A356 Al-Si alloy. *Journal of Materials Processing Technology*. 2006;174(1-3):371-83.
24. Meng Y, Cui J, Zhao Z, Zuo Y. Effect of vanadium on the microstructures and mechanical properties of an Al-Mg-

- Si-Cu-Cr-Ti alloy of 6XXX series. *Journal of Alloys and Compounds*. 2013;573:102-11.
25. Apelian D, Cheng JJ. Al-Si Processing variables: effect on grain refinement and eutectic modification. *AFS Transactions*. 1986;94:797-808.
26. Farahany S, Idris MH, Ourdjini A. Effect of bismuth and strontium interaction on the microstructure development, mechanical properties and fractography of a secondary Al-Si-Cu-Fe-Zn alloy. *Materials Science and Engineering: A*. 2015;621:28-38.
27. Eiken J, Apel M, Liang S-M, Schmid-Fetzer R. Impact of P and Sr on solidification sequence and morphology of hypoeutectic Al-Si alloys: Combined thermodynamic computation and phase-field simulation. *Acta Materialia*. 2015;98:152-63.
28. Lu S-Z, Hellawell A. The mechanism of silicon modification in aluminum-silicon alloys: Impurity induced twinning. *Metallurgical Transactions A*. 1987;18(10):1721-33.
29. Liao C, Chen J, Li Y, Tu R, Pan C. Morphologies of Al4Sr Intermetallic Phase and Its Modification Property upon A356 Alloys. *Journal of Materials Science & Technology*. 2012;28(6):524-30.
30. Shivaprasad CG, Aithal K, Narendranath S, Desai V, Mukunda PG. Effect of combined grain refinement and modification on microstructure and mechanical properties of hypoeutectic, eutectic and hypereutectic Al-Si alloys. *International Journal of Microstructure and Materials Properties*. 2015;10(3/4):274.
31. Cáceres CH. Microstructure Design and Heat Treatment Selection for Casting Alloys Using the Quality Index. *Journal of Materials Engineering and Performance*. 2000;9(2):215-21.
32. Tekmen C, Ozdemir I, Cocen U, Onel K. The mechanical response of Al-Si-Mg/SiCp composite: influence of porosity. *Materials Science and Engineering: A*. 2003;360(1-2):365-71.